Rotary Gallop in the Untethered Quadrupedal Robot Scout II

James Andrew Smith
Centre for Intelligent Machines
McGill University
Montréal, Canada
Email: jasmith@cim.mcgill.ca

Ioannis Poulakakis
Centre for Intelligent Machines
McGill University
Montréal, Canada
Email: poulakas@cim.mcgill.ca

***Abstract*— This paper discusses recent galloping results obtained using the Scout II quadrupedal robot, an underactuated robot with minimal sensing. The rotary variation of the gallop has been implemented, resulting in a motion which demonstrates both emergent stability and a circular trajectory, as predicted in earlier simulation studies by other researchers. It also demonstrates phase relationships in the leg touchdown pattern which resemble results from biology.**

I. Introduction

Groundbreaking work in the field of robot locomotion was achieved by Raibert in the 1980s at the CMU and MIT leg labs using dynamically stable one-, two- and four-legged robots, [1]. This work demonstrated that simple controllers could be made to stabilize high speed motion. Since then there have been many studies and implementations of various dynamic gaits on robotic platforms. Gaits such as the pronk, the trot and the bound have all received a fair amount of experimental and numerical study, [1], [2]. Although they have been studied in biological systems, [4], [6], and in simulation, [3], [5], [8], the half-bound and gallop gaits had not been implemented on any mechanical system until recently, [2], using the Scout II robot. This paper is a continuation of that work.

The gallop is a four-beat gait – that is, each of the four legs touches down on the ground sequentially. Two variations of the gallop are known to exist in the animal world: the transverse, in which the footfall pattern connects the front and rear lateral legs diagonally, and the rotary, in which the footfall pattern alternates between longitudinal and lateral throughout the stride, see Fig. 4.

Research that has looked at the gallop has pointed out interesting features that make it a worthwhile candidate for practical implementation on a robotic platform. These features include an emergent stability characteristic which may simplify control [3] (albeit for the transverse gallop constrained to the sagittal plane) and higher efficiency than other gaits at high speeds [4]. The potential of emergent gait stability opens up the possibility of a requirement for fewer and less expensive sensors to control a galloping robot. The out-of-phase nature of the gallop footfalls makes an investigation into its three-dimensional characteristics interesting, especially in terms of the roll and yaw characteristics which have been dismissed by some researchers [5] and emphasized by others [6].

Ringrose addressed the issue of galloping in [7], simulating both the rotary and transverse gallops in three dimensions, assuming a specific toe shape, similar to McMahon's model presented in [8], to achieve the galloping gait. Of note is the observation that Ringrose's rotary gallop resulted in a circular trajectory, which was also found in Scout II's rotary gallop.

Nanua presented interesting two- and three-dimensional simulations which illustrated transverse galloping using one rotary and one prismatic actuator per leg, [9] but without requiring a specific toe shape.

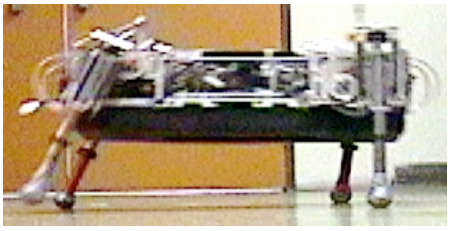

Fig. 1. Scout II: a galloping robot.

Both Nanua and Herr have argued that flexible spines and even necks are important features of at least the transverse gallop because of their presence in biological systems. In a minimal gallop system, though, these are not necessary as is evident by results found in [2].

At present, the next most relevant work on robotic galloping is being conducted at Ohio State and Stanford Universities. A number of simulations, mostly concentrating on the transverse gallop in the sagittal plane, [10], [5] have been conducted but, to the authors' best knowledge, no results of any galloping implementation have been published as of the time of this writing.

Unlike other gaits, the gallop has only been demonstrated to work on a single robot, Scout II. Although the gallop has been studied a number of times in simulation, it has mostly been from a two-dimensional perspective and through the use of models which contain more actuation than Scout II. This paper demonstrates that a minimally actuated robot, with no external sensing is capable of a stable rotary gallop, albeit in a circular trajectory.

II. The Scout II Quadrupedal Robot

The design of Scout II (refer to [11] for details) is an exercise in simplicity. An essential feature for real-world tasks is power autonomy, which imposes very strict design constraints. These features underline the importance of designing a platform using a minimum number of actuators and deriving controllers that have a minimum reliance on sensing.

Fig. 2 illustrates the Scout II model, consisting of a rigid body with four compliant prismatic legs. The angle of each leg with respect to the body's vertical axis is φ. A positive φ refers to the leg pointing towards the front of the robot, with respect to the direction of travel. Moving the leg forward requires the application of a positive hip torque. Other important variables and parameters, shown in Fig. 2 are the spring constant, k, damping constant, b, leg length, l and half hip spacing, L. Parameter values are found in Table I.

In marked contrast to other robot models in [3] and [9], which use two actuators per leg, Scout II uses only a single actuator per leg, located at the hip joint, which provides leg rotation in the sagittal plane. Each leg assembly consists of a lower and an upper leg, connected via a spring to form a compliant prismatic joint. Thus each leg has two degrees of freedom (DOF): the hip's rotational actuated DOF and the passive and compliant prismatic DOF. Each leg houses a linear potentiometer for determining ground contact, while each motor houses a quadrature encoder for measuring angle of the leg. Each motor amplifier outputs a measurement of motor current which is used to estimate applied hip torque.

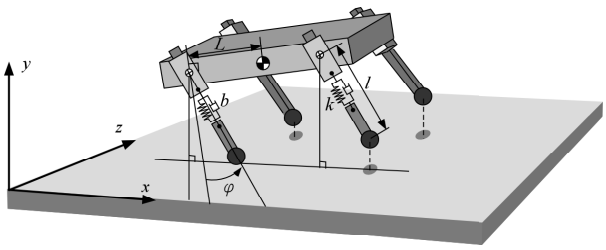

Fig. 2. Schematic diagram of Scout II galloping with one leg on the ground, illustrating important variables and parameters.

In the current configuration, the legs at the rear of the robot are identified as Leg 1 and Leg 3. The legs at the front of the robot, with respect to direction of travel, are Leg 2 and Leg 4, as is shown in Fig. 3. Leg 3 is arbitrarily chosen to be the "synchronization" leg which provides a reference for various measurements; the synchronization is based on the flight-to-stance transition of Leg 3. In this paper the term "step" refers to the completion of one back-and-forth (i.e. "retraction" and "protraction") motion of a leg, while "stride" refers to the motion of all four legs during the step of the synchronization leg.

Although conceptually simple, Scout II is a complex system exhibiting underactuated, highly nonlinear, intermittent dynamics. The complexity is further increased by the limited ability in applying hip torques due to actuator and friction constraints and by the existence of unilateral ground forces. These qualities explain why direct application of modern robot control theory had limited success in deriving controllers for dynamically stable legged robots. Despite this complexity the authors found that simple, Raibert-style control laws operating mostly in a feedforward fashion, with minimal sensing, can stabilize periodic motions, resulting in robust and fast sagittal plane running with a bounding gait, [12], [13]. Most importantly, the same simple, minimalist control approach can be used to excite and stabilize more complex nonsagittal, three-dimensional running gaits such as the rotary gallop. Experimental demonstration of this issue constitutes the central contribution of this paper.

TABLE I
Scout II Mechanical Parameters.

Body Mass	21.65 kg
Individual Leg Mass	0.97 kg
Leg Spring Compliance	4.3 kN/m
Body Length	0.837 m
Leg Length	0.323 m
Front Hip Width	0.498 m
Back Hip Width	0.413 m
Hip-to-hip length	0.552 m
Sprocket and belt transmission ratio	48/34
Sprocket and belt efficiency	96%
Motor Planetary Gear Ratio	72.38
Maximum Gear Efficiency	68%

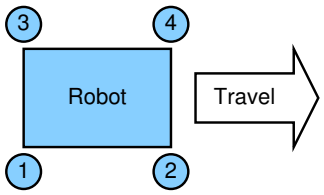

Fig. 3. Simplified bird's eye view of Scout II, illustrating direction of travel with respect to numbered leg layout. Here, Leg 1 and Leg 3 form the rear lateral pair while Leg 2 and Leg 4 form the front lateral pair.

III. The Rotary Gallop

The strategy for enabling the rotary gallop hinges on the idea that the bound is essentially a limiting case of the gallop in which the lateral leg pairs have no phase difference. By adding an offset in the touchdown angles of a lateral leg pair, the bounding motion is perturbed and a new motion with a different footfall pattern emerges. Appropriate selection of the offset angles results in the rotary gallop gait, without intensive control action reflecting the robot's natural dynamics that depend on its physical properties. This is also the method used to enable the half-bound, [2], which for all intents and purposes is also a "half-gallop".

As shown in Fig. 4 the foot touchdown sequence of the rotary gallop follows a pattern which encircles the centre

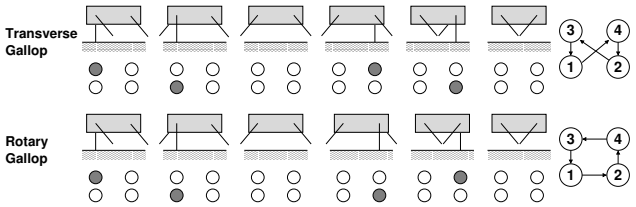

Fig. 4. The simplified footfall patterns of two four-beat gaits: transverse (top) and rotary (bottom) gallops. Cases in which more than one leg is on the ground are ignored for the sake of clarity.

of the body, whereas the transverse gallop's pattern criss-crosses the centre of the body. In the transverse gallop, the lead leg of both front and rear leg pairs is on the same side, whereas in the rotary gallop they are on opposite sides.

A. Controller Description

In this section a description of the control actions taken by the robot based on the leg states is presented. Each leg can find itself in one of three possible states, as shown in Fig. 5. During "stance" the leg is in contact with the ground via its toe, whereas in "flight" it is in the air. The stance phase is divided into the "stance-retraction" state, in which the leg moves backwards and the "stance-brake" state, wherein the leg is at its rear-most point, also known as the sweep-limit. It is important to mention that state changes are made based on input from only two sensor types: the legs' linear potentiometers and the leg motors' rotary encoders. The potentiometers are used to detect compression or decompression of the legs during the touchdown impact with or liftoff from the ground. The encoders allow state transition when the preassigned stance-brake angle is reached. In Fig. 5, τ refers to the hip torque, while φ^{td} and φ^{swl} are the leg angles for touchdown and sweep-limit, respectively. The desired torque during stance is τ_{des} and the proportional and derivative controller gains are k_P and k_D, respectively.

The cases below describe the control actions taken based on the legs' states, using only Leg 1 and Leg 3 as examples, and are also applicable to Leg 2 and Leg 4:

Case 1: Leg 1 and Leg 3 are both in flight. Leg 1 is actuated to a predetermined touchdown angle, whereas Leg 3 is actuated to a different touchdown angle to enforce separate touchdown times.

Case 2: Leg 1 and Leg 3 are both in stance. Both legs are swept back with a constant *desired* torque until they reach the stance-brake angle. Note, that applied torque is not constant, as described in Section IV.

Case 3: Leg 1 is in stance and Leg 3 is in flight. Leg 1 is commanded to move as it does in Case 2. Leg 3 is commanded to move as it does in Case 1.

Case 4: Leg 1 is in flight and Leg 3 is in stance. Leg 1 is commanded to move as outlined in Case 1. Leg 3 is commanded to move as in Case 2.

IV. Experimental Results

The objective for the experimental runs was to capture data over a large number of galloping strides which could demonstrate that the gallop was, in fact, stable and repeatable. Touchdown leg angles were set in order to have Leg 3, the synchronization leg, touchdown first, followed by Leg 1, Leg 2 and then Leg 4.

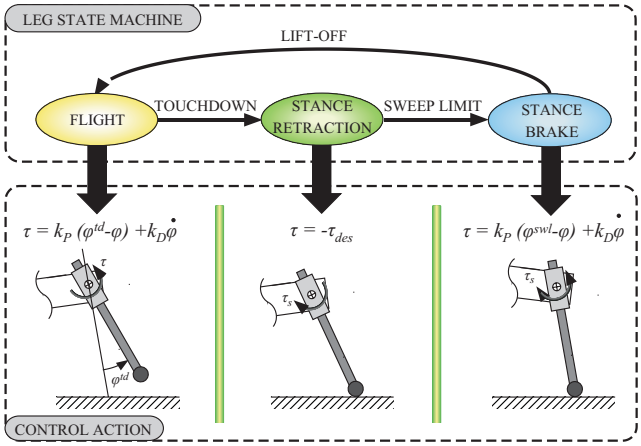

Fig. 5. The leg state machine, including equations for torque for each state. Parameter values are described in Table II.

In each of the ten trials conducted, the robot was first made to bound forward in a straight line, accelerating for a number of strides before the gallop behaviour was commanded. During the bounding phase, the robot was made to accelerate by increasing touchdown angles by one degree per stride, between the limits shown in Table II. Values for other controller set points are also found in this table.

TABLE II
Controller Parameter Values.

Leg #	φ^{td} (^{o}) Bound	φ^{td} (^{o}) Gallop	τ_{des} (Nm)	k_P Flight	k_P Stance	k_D
1	10-17	17	45	250	300	5
2	12-19	19	45	250	300	5
3	10-17	19	45	250	300	5
4	12-19	21	45	250	300	5

Once the bound had finished accelerating, the gallop was commanded and the touchdown angles on Leg 3 and Leg 4 were increased by two degrees, to 19 and 21 degrees, respectively, while Leg 1 and Leg 2 maintained touchdown angles of 17 and 19 degrees, respectively. At this point the robot began to turn counter-clockwise in a circle whose circumference varied from approximately seven to nine meters. The circumference of the circle covered by the robot was estimated using visual markers on the floor which outlined circles of varying radii. A handheld stopwatch was used to record the length of time it took the robot to make a complete circle, starting at the point at which the gallop command was issued.

A typical sequence of experimental footfalls is illustrated in Fig. 6. The overview portion captures the consistency of the gaits produced during the trials. The detailed view from Fig. 6 shows that the "duty cycle", or ratio of stance time to stride period, is consistently less than 50% for each leg.

Leg angles, leg angular velocity and applied hip torque are presented in Figs. 7, 8 and 9, respectively. In each plot, the stance and flight states are also illustrated for reference purposes. For the sake of clarity, the stance-brake state is not illustrated, rather it is added to the end of the stance state.

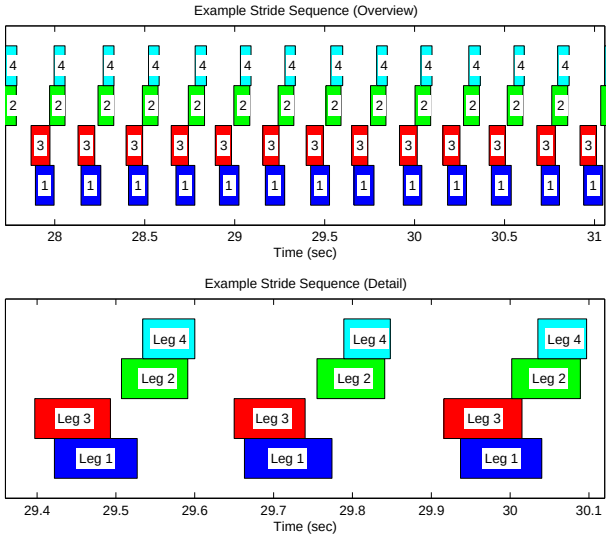

Fig. 6. Illustration of the overview (top) and detailed view (bottom) of a typical experimental rotary gallop footfall sequence. Filled boxes represent the time that a given leg touches the ground (i.e. stance); areas in the sequence outside the boxes represent time that the leg spends in flight.

A few changes have been made since the results published in [2] where the robot's touchdown angles were fixed to those desired for the galloping motion throughout the experiment, including during startup. Although the robot tended to settle into repeatable cyclical motion, this was not always the case. By initializing the motion with a stable bound and perturbing it with new touchdown angles the robot settled into a repeatable rotary gallop gait. Furthermore, as opposed to using a largely different pair of touchdown angles (17 and 32 degrees), as in [2], the current results used touchdown angles which varied from the bounding angles by only two degrees. Not only was the resulting motion more repeatable, it was also much faster than experimental gallop results using the previous settings.

It is worth mentioning that Scout II has previously demonstrated the ability to turn while bounding using differential torques in the two longitudinal leg pairs, [14]. The application of differential torque has also been used previously to straighten out the bounding motion of Scout II since it has a tendency to veer counter-clockwise.

Fig. 10 shows the leg angular speed as a function of the applied motor torque in an experimental galloping run for all four legs. In reading Fig. 10 note that, according to the sign conventions shown in Fig. 2, during stance-retraction the motors operate in the third quadrant while during flight they operate in the first quadrant (positive torques correspond to the leg moving forward). Careful inspection of Fig. 10 reveals that the motors are saturated most of the time during the stance-retraction phase. This characteristic

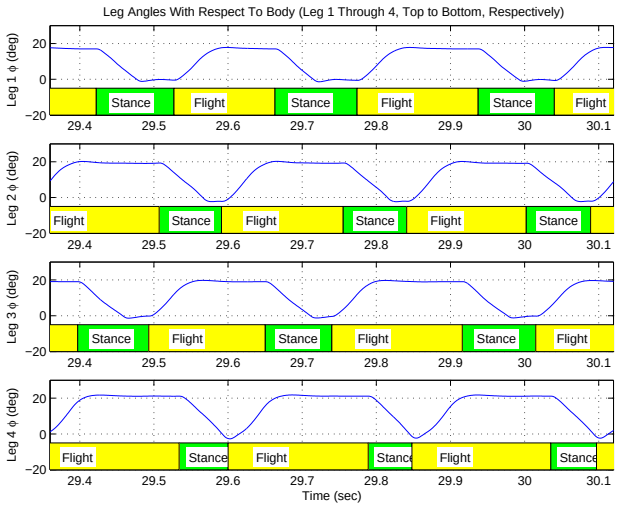

Fig. 7. Angles of the legs with respect to the body's vertical axis, starting with Leg 1 (top) and ending with Leg 4 (bottom). The state of the leg, derived from a linear potentiometer in the leg, is illustrated on each graph.

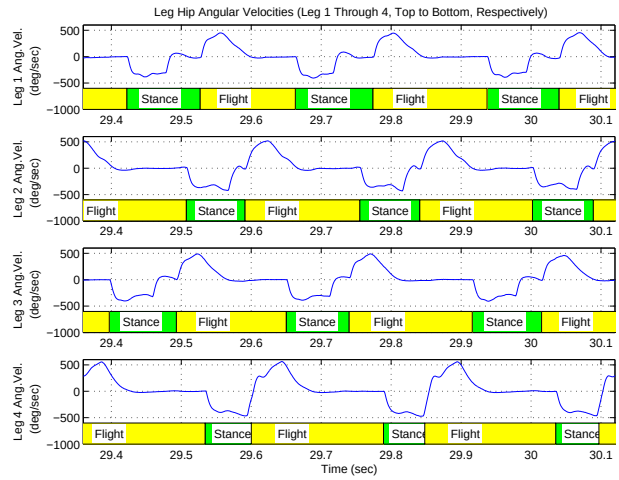

Fig. 8. Angular velocities of the legs, starting with Leg 1 (top) and ending with Leg 4 (bottom). The state of the leg, derived from a linear potentiometer in the leg is illustrated on each graph.

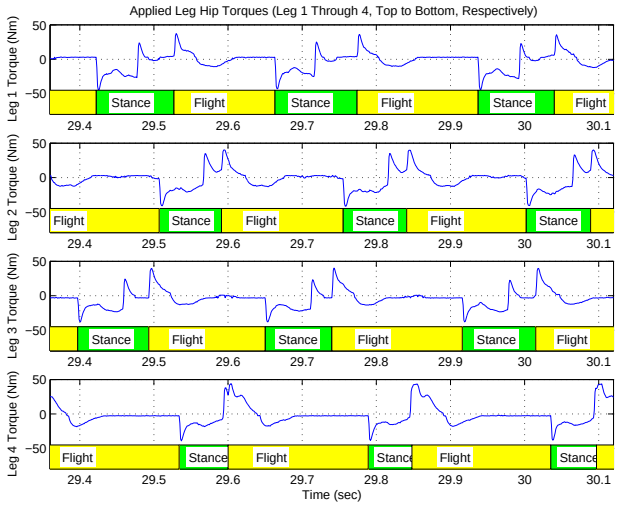

Fig. 9. Torques applied at the hips, starting with Leg 1 (top) and ending with Leg 4 (bottom). The state of the leg, derived from a linear potentiometer in the leg is illustrated on each graph.

has also been observed in other dynamic gaits, such as the bound, see [12], and has a significant effect on the motion. Fig. 10 clearly demonstrates the limited control afforded during the stance phase and reveals the severe constraints that more elaborate feedback-based controller must take into account in order to be successfully implemented in experiments. Note also that similar behaviour is observed in all four legs, the exception being the fourth quadrant of the Leg 4. This discrepancy is attributed to the short stance duration of Leg 4 which results in the lift-off coming slightly after the sweep limit event, thus the sweep limit controller does not have enough time to brake the leg.

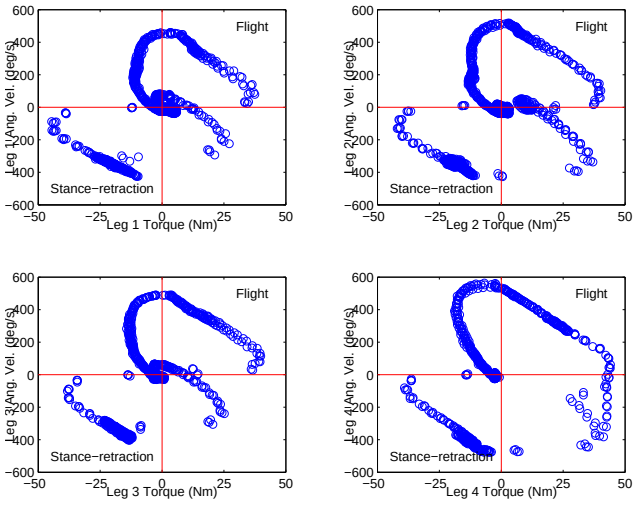

Fig. 10. Individual motor speed-torque curves illustrating the performance limits under which the motors and associated amplifiers operate.

For mobile robots to be of practical utility, they need to be energy efficient and be able to operate in a power autonomous fashion for extended periods of time. An increasingly accepted measure of energy efficiency is the specific resistance - a measure originally proposed by Gabrielli and von Karman, [15],

$$\epsilon(v) = \frac{P(v)}{mgv}$$

where P is the power expenditure, m is the mass of the vehicle, g is the gravitational acceleration constant, and v is the vehicle speed. Since many vehicle specific resistances quoted in the literature are based on the average mechanical output power of the actuators, this has been calculated as a function of speed, see Fig. 11. Even though energy efficiency has so far not been optimized, Scout II at top galloping speed achieves a relatively low specific resistance based on mechanical power, equal to 0.5, somewhat higher than previous bounding results. Specific resistance based on electrical power consumption, 1.7, is also somewhat higher than previous bounding results, as can be seen in Fig. 11.

To generalize the results presented above for one stride and to demonstrate consistency in different strides, ten experimental runs were performed containing 190 strides.

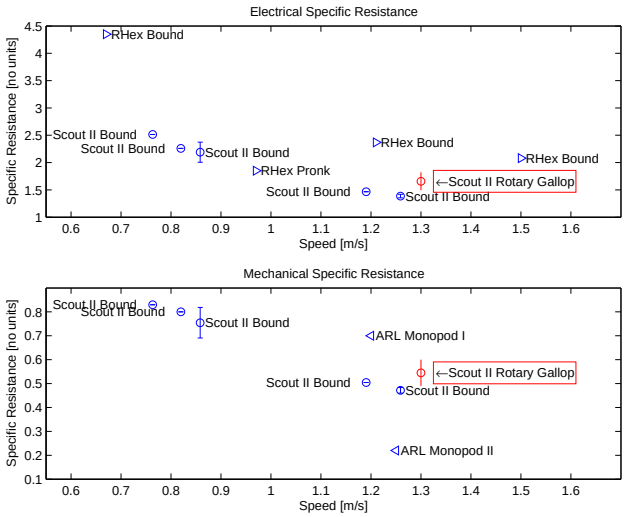

Fig. 11. Electrical (top) and mechanical (bottom) specific resistance measurements in comparison with RHex [16], Scout II (bounding) and the ARL Monopod [17].

Three strides (1.6% of the total) were discarded from the data. One was discarded because it violated the requirement that the synchronization leg, Leg 3, be first to touchdown. Two strides were discarded because at least one leg had a stance time which lasted less than 70% of the average stance time for that leg. The comparison of different strides is undertaken using discrete locomotion variables such as duty cycle and phase difference, which characterize the stride. A summary of these variables is found in Table III.

TABLE III
EXPERIMENTAL RESULTS FOR 10 RUNS, 187 STRIDES TOTAL.

Variable	Mean	Std. Dev.
Stride Period	0.259	0.014
Speed	1.3 m/s	0.1 m/s
Mech. Spec Resistance	0.5	0.1
Elec. Spec. Resistance	1.7	0.2
Duty Cycle, Leg 1	0.409	0.022
Duty Cycle, Leg 2	0.330	0.025
Duty Cycle, Leg 3	0.375	0.028
Duty Cycle, Leg 4	0.243	0.018
Phase Diff, Leg 1	0.070	0.026
Phase Diff, Leg 2	0.408	0.039
Phase Diff, Leg 3	0	0
Phase Diff, Leg 4	0.508	0.036

V. DISCUSSION

In previous – mainly bounding – experiments, [12], [13], Scout II used a leg spring constant of about 3500 N/m, which resulted in large leg compression (nearly 10 cm), approaching or contacting the mechanical stops on the legs. As explained in [7], a higher spring constant results in a higher stride frequency (about 3.5 Hz in the bound with 3500 N/m springs, vs. about 3.9 Hz in the gallop with 4300 N/m springs), allows a reduction in stance time and also

a higher steady-state velocity. The higher spring constant used for this work ensured that the leg compression was much less (often less than 6 cm). The end result is that unlike in the previously reported work, [2], the galloping motion was more energetic, demonstrating significant toe clearance during phases of the motion where all legs are off the ground.

Despite the fact that the galloping controller has not yet been optimized for speed, it is slightly faster than the bounding controller, with bounding resulting in speeds up to 1.3 m/s, while galloping results in up to 1.4 m/s. Power consumption on the robot is significantly higher than in previously conducted bounding experiments. Whereas mean electrical power consumed by the robot during a bound varied between 430 and 440 Watts, the mean power consumption during the rotary gallop is about 515 Watts, an increase of over 15%, with only a small corresponding increase in speed, indicating a lower efficiency.

The phase relationships between the synchronization and other legs results in values which are very similar to those found by Alexander in [18], as is shown in Fig. 12. In both cases there is a 10% (with respect to stride period) phase shift between legs in each lateral pair. The only significant difference between the two cases is that the third leg to touchdown in Alexander's case does so somewhat later (corresponding to a 10% phase shift) than on Scout II.

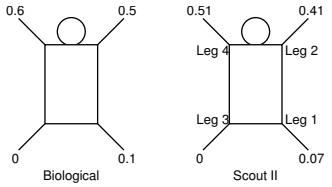

Fig. 12. A typical rotary gallop phase relationship in a biological system (left, adapted from [18]) versus that found on Scout II (right).

Although it is not currently possible to measure directly, postural variables (roll, pitch, yaw, COM height) all converge to stable, repeatable patterns, as can be deduced from the regular footfall pattern evident in Fig. 6 as well as the repeatable circular trajectory of the robot on the floor. Moreover, the simplicity of the controller's structure and its success in producing a stable rotary gallop contributes to the increasing evidence that complex behaviours can be stabilized via simple control laws. The results presented in this paper experimentally demonstrate related findings, [3], which showed that gait stability was an emergent property of a transverse galloping model.

In addition, the fact that the robot gallops in a circle is not entirely unexpected as it agrees with the results for the rotary gallop simulation found in [7], which compares a galloping quadruped to two bipeds which each have a tendency to creep laterally. Because the lead legs for the two bipeds on are opposite sides, the opposing lateral motion results in a yawing moment. Changing direction of rotation as well as galloping on non-flat terrain is left for future work.

VI. Conclusion

One of the more remarkable aspects of this research is that the motion of an underactuated robot and minimally sensing robot such as Scout II can be made to converge to a stable and repeatable rotary gallop. This experimentally confirms earlier simulated results, [3], which identified emergent stability as a characteristic of the gallop, albeit for the transverse variety constrained to the sagittal plane. These experiments also confirm simulated findings found in, [7], that the rotary gallop has a tendency to result in circular trajectories. In addition, the phase relationships found in the touchdown pattern closely resembles results from the biological world, as found in [18].

Acknowledgments

The authors thank Dr. M. Buehler for getting our work started and Michelle Huth for help with recent experiments.

References

[1] Marc Raibert. *Legged Robots That Balance*. The MIT Press, 1986.

[2] I. Poulakakis, J. A. Smith, and M. Buehler. On the dynamics of bounding and extensions towards the half-bound and the gallop gaits. In *Proceedings of the 2nd International Symposium on Adaptive Motion of Animals and Machines (AMAM)*, pages 453–458, March 2003.

[3] Hugh M. Herr and Thomas A McMahon. A galloping horse model. *International Journal of Robotics Research*, 20:26–37, January 2001.

[4] D. F. Hoyt and C. R. Taylor. Gait and the energetics of locomotion in horses. *Nature*, 292:239–240, 1981.

[5] D. W. Marhefka and D. E. Orin. Fuzzy control of quadrupedal running. In *Proceedings of IEEE International Conference on Robotics and Automation*, pages 3063–3069, San Francisco, CA, April 2000. IEEE International Conference on Robotics and Automation.

[6] Milton Hildebrand. Analysis of asymmetrical gaits. *Journal of Mammalogy*, 58(2):131–156, May 1977.

[7] Robert Ringrose. *Self-Stabilizing Running*. PhD thesis, MIT, 1996.

[8] T.A. McMahon. The role of compliance in mammalian running gaits. *Journal of Expermental Biology*, 115, 1985.

[9] Prabjot Nanua. *Dynamics of a Galloping Quadruped*. PhD thesis, Ohio State University, 1992.

[10] J. P. Schmiedeler, D. W. Marhefka, D. E. Orin, and K. J. Waldron. A study of quadruped gallops. In *Proceedings of 2001 NSF Design, Service, and Manufacturing Grantees and Research Conference*, Tampa, FL, January 2001. NSF Design, Service, and Manufacturing Grantees and Research.

[11] Robert Battaglia. Design of the Scout II quadruped with preliminary stair climbing. Master's thesis, McGill University, May 1999.

[12] I. Poulakakis, J. A. Smith, and M. Buehler. Experimentally validated bounding models for Scout II quadrupedal robot. In *Proceedings of the International Conference on Robotics and Automation*, New Orleans, LA, USA, April 2004. IEEE. In Press.

[13] S. Talebi, I. Poulakakis, E. Papadopoulos, and M. Buehler. *Experimental Robotics VII*, chapter Quadruped Robot Running with a Bounding Gait, pages 281–289. Lecture Notes in Control and Information Sciences. Springer-Verlag, 2001.

[14] D. Papadopoulos and M. Buehler. Stable running in a quadruped robot with compliant legs. In *Int. Conf. on Robotics and Automation (ICRA)*, pages 444–449, California, 2000. IEEE.

[15] G. Gabrielli and T. H. von Karman. What price speed? *Mechanical Engineering*, 72(10), 1950.

[16] D. Campbell and M. Buehler. Preliminary bounding experiments in a dynamic hexapod. In B. Siciliano and P. Dario, editors, *Experimental Robotics VIII*, volume 5 of *Springer Tracts in Advanced Robotics*, pages 612–621. Springer-Verlag, 2003.

[17] M Ahmadi and M. Buehler. The ARL Monopod II running robot: Control and energetics. In *IEEE Int. Conf. Robotics and Automation*, pages 1689–1694, Detroit, Michigan, USA, May 1999.

[18] R. McNeill Alexander. The gaits of bipedal and quadrupedal animals. *International Journal of Robotics Research*, 3(2):49–59, Summer 1984. Special Issue: Legged Locomotion.